Neuropharmacology 56 (2009) 984–993

Contents lists available at ScienceDirect

Neuropharmacology

journal homepage: www.elsevier.com/locate/neuropharm

Block of voltage-gated calcium channels stimulates dopamine efflux in rat mesocorticolimbic system

Francesco Belardetti [a,1], Soyon Ahn [a,1], Kitty So [b], Terrance P. Snutch [b,c], Anthony G. Phillips [b,*]

[a] Neuromed Pharmaceuticals Inc., Suite 301-2389 Health Sciences Mall, Vancouver, BC, Canada V6T1Z3
[b] Department of Psychiatry, 2255 Wesbrook Mall, University of British Columbia, Vancouver, BC, Canada V6T2A1
[c] Michael Smith Laboratories, Rm 219–2185 East Mall, University of British Columbia, Vancouver, BC, Canada V6T1Z4

ARTICLE INFO

Article history:
Received 8 November 2008
Received in revised form
31 January 2009
Accepted 2 February 2009

Keywords:
Dopamine
Mesocorticolimbic system
GABA
NP078585
Voltage-gated calcium channel
Drug dependency
Microdialysis

ABSTRACT

Dopamine (DA) efflux from terminals of the mesocorticolimbic system is linked to incentive motivation, drug dependency and schizophrenia. Strategies for modulating dopaminergic activity have focused on transmitter receptors or the DA transporter, not on DA release, largely due to lack of systemically available drugs acting at this level. Central synapses use two main calcium channels for excitation–secretion coupling, either P/Q-type, N-type, or both. Here we investigate changes in mesocorticolimbic DA efflux following administration of NP078585, a novel orally available calcium channel blocker exhibiting high affinity block of N- and T-types versus P/Q- and L-types. NP078585 was applied either intra peritoneally (i.p.; 2.5–10 mg/kg) or by reverse-dialysis (10–25 μM) into either the Ventral Tegmental Area (VTA) or the Nucleus Accumbens (NAc), and the changes in DA levels in both the VTA and NAc were monitored using microdialysis. We found that both systemic and central administration of NP078585, but not vehicle, enhanced DA efflux in the NAc but not the VTA. The enhancement of DA levels was replicated by local applications of ω-conotoxin GVIA (2.5 μM), a selective peptide N-type channel blocker, to either VTA or NAc, suggesting N-type mediation. Furthermore, application of the $GABA_A$-selective antagonist bicuculline (50 μM) to the VTA enhanced DA efflux in both VTA and NAc, and occluded the NP078585-induced enhancement in the latter structure. We propose that the actions of NP078585 and ω-conotoxin largely reflect block of N-type channels in terminals of GABAergic interneurons, leading to reduced GABA release, disinhibition of DA neurons and enhanced DA release in the NAc.

1. Introduction

The mesocorticolimbic dopaminergic system projects from the VTA in the midbrain to limbic and cortical areas (Fallon and Moore, 1978). This system plays a central role in learning and motivation (Fibiger and Phillips, 1988; Schultz, 2007), whereas its aberrant activity is causally related to drug dependency and schizophrenia (Koob, 1992; Kupfermann et al., 2000; Kandel, 2000). Available pharmacotherapies acting on this system are only partially effective and have substantial side effects. In this regard, novel drugs modulating neural activity and transmitter release within the mesocorticolimbic system may produce effective treatments for psychoses and drug dependency. Voltage-gated calcium channels may constitute novel targets for the therapeutic control of dopaminergic mechanisms because of their roles in coupling membrane depolarization to neurotransmitter release, as well as in shaping neuronal excitability and firing patterns (Catterall, 2000; Perez-Reyes, 2003). However, until recently this hypothesis could not be tested directly, due to a lack of appropriate CNS-penetrant blockers.

Voltage-gated calcium channels have been classically divided between high-voltage activated (HVA; P, Q, R, L- and N-types) and low-voltage activated channels (LVA, T-type; Catterall, 2000; Perez-Reyes, 2003; Snutch et al., 2005). Primary candidates for the regulation of DA release are the HVA N- and P/Q-type channels. N-type channels are largely restricted to the CNS, where alone or in combination with P/Q-type channels couple neuronal depolarization to transmitter release (Dunlap et al., 1995). Both gene knockout and pharmacological experiments have clearly implicated N-type channels in ethanol dependency (Newton et al., 2004, 2008), potentially linking N-type channels to regulation of DA release.

LVA T-type channels are widely distributed within the CNS and may also play an important role in DA release (Perez-Reyes, 2003).

* Corresponding author. Department of Psychiatry and Institute of Mental Health, University of British Columbia, 2255 Wesbrook Mall, Vancouver, Canada, BC V6T 2A1. Tel.: +1 604 822 4624; fax: +1 604 822 7756.
E-mail address: aphillips@psych.ubc.ca (A.G. Phillips).
[1] These authors contributed equally to this article.

0028-3908/$ – see front matter © 2009 Elsevier Ltd. All rights reserved.
doi:10.1016/j.neuropharm.2009.02.001

Functionally, T-type channels support bursting action potential activities, as first observed in thalamic GABAergic neurons (Huguenard and Prince, 1992). Furthermore, GABAergic neurons are central to the control of mesocorticolimbic DA neurons (Johnson and North, 1992). While it is not known whether T-type channels shape the excitability of mesolimbic GABAergic neurons, they support the slow pace-maker activity linked to tonic dopaminergic release in a subset of nigral dopaminergic neurons (Wolfart and Roeper, 2002).

N-type channels have a clearly established role in mediating chronic and inflammatory pain signaling (reviewed by Snutch, 2005), promoting an intense effort to develop orally available, potent and selective N-type channel blockers (Snutch et al., 2001b). As part of this effort, Neuromed Pharmaceuticals has developed NP078585, a use- and state-dependent blocker of N- and T-type, but not P/Q-type or L-type channels that suppresses chronic neuropathic and inflammatory pain in rodents after oral administration (Snutch et al., 2001a, 2003). Recently, NP078585 has been shown to reduce ethanol-induced reinforcement and reward, and stress-induced reinstatement of ethanol seeking (Newton et al., 2008). Here we have used NP078585 and the N-type peptide antagonist, ω-conotoxin GVIA, as tools to investigate the role within the VTA and NAc of N- and T-type calcium channels in DA efflux from dendrites and axon terminals, as sampled by microdialysis in freely moving rats. Preliminary data from this study were presented in abstract form (Vacca et al., 2005).

2. Methods

All experimental protocols were approved by the Committee on Animal Care, University of British Columbia and conducted in compliance with guidelines provided by the Canadian Council of Animal Care.

2.1. Drugs and preparation

NP078585 (previously named NMED-126) was obtained from Neuromed Pharmaceuticals (Vancouver, British Columbia, Canada). NP078585 [1-(6,6-bis(4-fluorophenyl)hexyl)-4-(3,4,5-trimethoxybenzyl)piperazine; Fig. 1] blocks N-type calcium channels *in vitro* with an IC_{50} of ~110 nM, and $Ca_v3.1$, $Ca_v3.2$ and $Ca_v3.3$ T-type channels with IC_{50} values of ~200 nM, ~520 nM and ~250 nM, respectively. NP078585 blocks P/Q and L-type calcium channels with IC_{50} values of 1450 and 2810 nM, respectively. The detailed characterization of NP078585 is being published separately.

ω-Conotoxin GVIA was obtained from Alomone Labs (Jerusalem, Israel). Bicuculline methochloride, haloperidol, bovine serum albumin (BSA), dimethyl sulfoxide (DMSO) and polyethylene glycol 400 (PEG-400) were obtained from Sigma–Aldrich (Oakville, Ontario, Canada). All drugs' solutions were prepared daily approximately 30–60 min prior to injection or application by reverse-dialysis. NP078585 for systemic injections was prepared in 100% PEG-400. Drugs applied by reverse-dialysis (NP078585, haloperidol, bicuculline and cocktail combinations) were prepared in artificial Cerebro-Spinal Fluid (aCSF: 147.0 mM NaCl, 3.0 mM KCl, 1.0 mM $MgCl_2$ and 1.2 mM $CaCl_2$ in 10.0 mM sodium phosphate buffer, pH 7.4) containing 0.5% DMSO. ω-Conotoxin was prepared in aCSF containing 0.1% BSA.

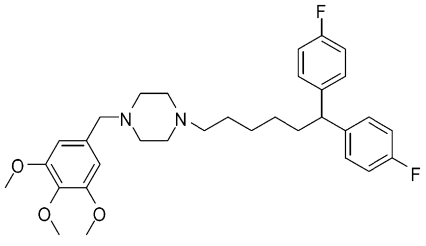

Fig. 1. Structural formula of NP078585. NP078585 [1-(6,6-bis(4-fluorophenyl)hexyl)-4-(3,4,5-trimethoxybenzyl)piperazine] is a distant derivative of the calcium channel blocker flunarizine.

2.2. Subjects and surgery

Sprague–Dawley male rats (weighting 250–275 g) were obtained from Charles River (St. Constant, Quebec, Canada) and housed in pairs upon arrival, then housed individually following surgery. The colony was maintained at ~21 °C with a 12 h light/dark cycle (lights on at 6 P.M.). Rats had free access to rat chow and water in home cages and testing chambers.

On the day of surgery, rats were anesthetized using 4% isoflurane (AErrane, Baxter Co., Toronto, Canada) mixed with oxygen, and then maintained with 2.0–2.5% isoflurane for the remainder of the surgery. Rats were placed on a heating pad to counter the hypothermic effects of isoflurane anesthesia. Subjects were placed in a stereotaxic apparatus in flat skull position (mouth bar at −3.2 mm). All coordinates were determined using the atlas of Paxinos and Watson (1997). Each rat was implanted with two stainless steel guide *cannulae* (19 gauge × 15 mm) directly above the VTA [from bregma in mm, −5.8 anterio-posterior (AP), ±0.6 medio-lateral (ML); from dura in mm, −1.0 dorso-ventral (DV)] and NAc (+1.7 AP, ±1.1 ML, −1.0 DV)]. Rats received a subcutaneous injection of an analgesic (ketoprofen 0.05 ml or buprenorphine 0.1 ml) and allowed to rest under a heating lamp. Rats were allowed to recover from surgery for a minimum of 1 week prior to serving as subjects in the microdialysis experiments.

2.3. Microdialysis experiments

Microdialysis probes were assembled 1–2 days prior to microdialysis experiments. Probes were concentric in design with silica inlet–outlet lines. The dialysis surface consisted of a hollow semi-permeable membrane 1 or 2 mm in length (340 μm outer diameter; 65 kD molecular weight cut-off; Filtral 12; Hospal, Neurnberg, Germany). Typical *in vitro* probe recovery of an external DA standard was 18 ± 1% at room temperature.

The day prior to microdialysis experiments, probes were connected to an Instech dual-channel liquid swivel (Plymouth Meeting, PA) and flushed with aCSF. Following DA recovery tests, 2 mm probes were implanted in the NAc (+1.7 AP, ±1.1 ML, dialysis membrane spanned −6.0 to −8.0 DV) and 1 mm probes in the VTA (−5.8 AP, ±0.6 ML, −6.9 to −7.9 DV). Rats remained in the testing chamber overnight (14–16 h) while aCSF continuously perfused the probes at 1 μl/min. The next morning microdialysate samples were collected at 10 min intervals and assayed for DA content within 1 min. of collection Once baseline levels of DA were determined to be stable for four consecutive samples (less than 10% fluctuation), rats were administered NP078585, ω-conotoxin, haloperidol or bicuculline, alone or in combination, by systemic injection or reverse-dialysis. Nine additional microdialysis samples were collected at 10 min intervals before terminating the experiment.

2.4. High-pressure liquid chromatography

Microdialysis samples were analyzed immediately after collection using high-pressure liquid chromatography (HPLC) with electrochemical detection. Two systems were used, each consisting of an ESA 582 pump (Bedford, MA, USA), a pulse damper (Scientific Systems Inc., State College, PA), a Rheodyne Inert manual injector (model 7725i, 20 μl injection loop; Rohnert Park, CA), a Tosoh Bioscience Super ODS TSK column (2 μm particle, 2 mm × 10 mm; Montgomeryville, PA) an Antec Leyden Intro Electrochemical detector and VT-03 flow cell with a Ag/AgCl reference electrode ($V_{applied} = +650$ mV; Leyden, The Netherlands). The mobile phase [100 mM sodium acetate buffer, 40 mg/l EDTA and 4 mg/L of sodium dodecyl sulfate (variable between 3.5 and 4.5 mg/l), pH 4.1, 10% methanol] flowed through the system at 0.17 ml/min. EZChrome Elite software (Scientific Software, Pleasanton, CA) was used to acquire and analyze chromatographic data. The overall basal concentration of DA was significantly higher in the in the NAc (1.32 ± 0.14 nM) than in the VTA (0.35 ± 0.04 nM) [$F(1, 214) = 39.163$, $p < 0.001$].

2.5. Histology

Following microdialysis experiments, rats were sacrificed after being deeply anesthetized with isoflurane. Brains were promptly removed and stored in 20% w/v sucrose and 4% v/v paraformaldehyde solution for 5–7 days. Brains were then sliced into 50 μm coronal sections, stained with cresyl violet and examined for verification of probe placement.

2.6. Statistical analyses

Neurochemical data were normalized as the ratio to the mean value of the last four baseline samples (i.e., each data point was divided by the mean baseline value). Data shown in figures represent mean + Standard Error of the Mean (SEM). Statistical analysis involved a one-way repeated measures or two-way repeated measures Analysis Of Variance (ANOVA) with Time as the within-subject factor and treatment condition as the between-subjects factor. This was followed, when appropriate, by multiple comparisons of cell means using the Holm–Sidak test (at $p < 0.05$). For within-group comparisons, the final baseline data point was used as the control value. Between-groups analyses compared the summed values of Time points 5–7 of

each drug group against the vehicle group (i.e., dose response). All statistical analyses were performed using Sigmastat statistical software (Golden, CO).

2.7. Pharmacokinetics of NP078585

Brain and plasma level measurements following i.p. administration of NP078585 were performed by MDS Pharma Services (Bothell, WA). Briefly, 12 male Sprague–Dawley rats (weight range: 200–400 g) were fasted overnight prior to use. Following i.p. compound administration ($n = 6$ rats with 2.5 mg/kg and $n = 6$ with 10 mg/kg, in 100% PEG-400), blood samples (approximately 400 μL) were collected in lithium heparin by cardiac puncture from three rats at each time point (0.5 and 1 h) and dose, and immediately placed in ice prior to centrifugation. Both the size of the doses of NP078585 and the timing for sample collection (plasma and brain) for this pharmacokinetic study were selected to bracket the microdialysis data with DA, not to provide a one-to-one match between these two sets of data. Moreover, considering that the same animals were used for both plasma and brain measurements of the levels of NP078585 and the time required to collect the plasma samples and the brains, a 10-min resolution in the pharmacokinetic profiling (like that used for the DA sampling) would have been difficult to achieve. A 50 μL aliquot of plasma from each sample was transferred to dry ice for storage. Brains were collected immediately after obtaining the blood samples, washed with saline, and placed in individual tubes in dry ice. Levels of NP078585 in each plasma and brain sample were determined by LC–MS/MS. The HPLC system used for method development comprised an Agilent 1100 pump (Santa Clara, CA) with a Gilson 233XL autosampler (Middleton, WI), an Agilent Zorbax Eclipse XDB-C8 analytical column, whereas the HPLC for the assay standard method employed a Cohesive TLX (LX-mode) system (Franklin, MA) with an Agilent Zorbax Eclipse XDB-C18 column. Both HPLC systems used AB analyst software version 1.4.1, 5 μL injection volume, two solvent systems for the mobile phase, "A" [95/5% (v/v) water/acetonitrile, 0.1% formic acid] and "B" (acetonitrile, 0.1% formic acid), and an API-4000QTRAP mass spectrometer (Applied Biosystems, Foster City, CA) with ESI positive ionization mode.

We did not attempt to measure the levels of NP078585 achieved in the VTA, NAc or other brain regions during microdialysis experiments because of the uncertainties associated with these measurements (due to the detection limits of the analytical method, small amounts of tissue involved, sharp gradient of concentration around the probe).

3. Results

3.1. Effects of systemic NP078585 on mesocorticolimbic DA efflux

We first determined the i.p. doses of NP078585 that would produce brain levels sufficient to block N- and T-type calcium channels, as well as the time-course of these blocking actions. In separate experimental groups, the compound was delivered at 2.5 and 10 mg/kg and its plasma and brain concentrations measured at different time points. The i.p. injection of NP078585 at 2.5 mg/kg yielded a plasma concentration of 251 nM after 0.5 h ($n = 3$, range 166–315 nM), 63 nM at 1 h ($n = 3$, 13–128 nM) and finally 62 nM at 3 h ($n = 3$, 37–92 nM). In the same rats, the brain concentration of NP078585 reached after 0.5 h was 51 nM ($n = 3$; range: 37–61 nM), after 1 h 46 nM ($n = 1$) and after 3 h it was below quantitation level ($n = 3$). I.p. administration of NP078585 at 10 mg/kg resulted in plasma levels of 587 nM after 0.5 h ($n = 3$, range 86–1025 nM), 245 nM after 1 h ($n = 3$, 81–552 nM) and 233 nM after 3 h ($n = 3$, 182–309 nM). In the same subjects, brain levels after 0.5 h were 287 nM ($n = 2$; range: 183–391 nM), after 1 h 329 nM ($n = 1$) and 130 nM after 3 h ($n = 3$, 113–145 nM).

Using these doses as guidance for obtaining effective block of N- and T-type calcium channels (compared to the IC_{50}s – see Section 2), we next explored the effects of i.p. adiministration of NP078585 on spontaneous DA efflux within the dopaminergic mesocorticolimbic system. Each rat was chronically implanted with two microdialysis probes, one positioned in the NAc and the other in the VTA (Fig. 6). Microdialysis samples were collected continuously from each probe in awake, freely moving animals. After establishing a stable baseline for 40 min, NP078585 was injected i.p., using PEG-400 at 1 ml/kg as vehicle. At a dose of 2.5 mg/kg NP078585, the spontaneous efflux of DA from the NAc initially increased by more than 60% and then slowly declined, approaching the baseline approximately after 1.5 h (Fig. 2A). When the NP078585 dose was increased to 5 mg/kg, DA efflux from NAc further increased to about 80% of baseline. At 10 mg/kg NP078585

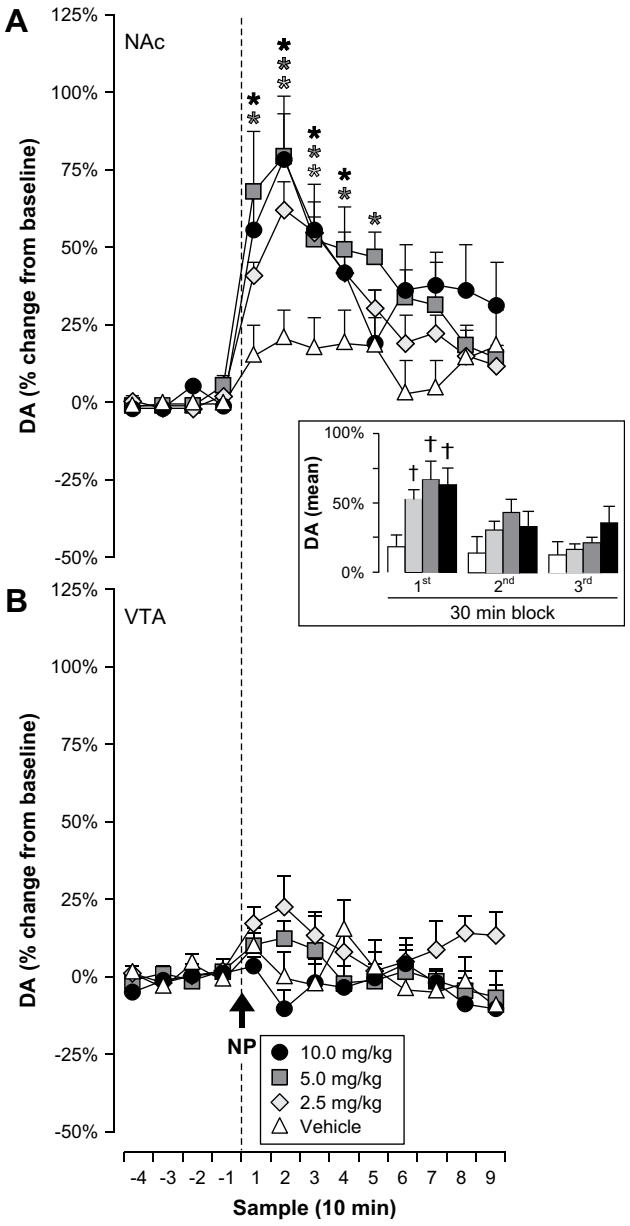

Fig. 2. Time-course of the change of DA efflux simultaneously measured by reverse-dialysis from both the NAc (A) and the VTA (B), before and after i.p. injections of NP078585 or vehicle (NP, arrow and vertical dashed line). The DA content from the samples, each collected at 10 min intervals, is expressed as percentage change from the baseline. The four experimental groups include vehicle alone (PEG-400 at 1 ml/kg, empty triangles; $n = 8$ rats for NAc data, $n = 6$ rats for VTAs) and NP078585 at 2.5 mg/kg (light grey diamonds; $n = 7$ for both sites), 5 mg/kg (dark grey squares; $n = 6$ NAc, $n = 8$ VTA), 10 mg/kg (black circles; $n = 7$ NAc, $n = 4$, VTA) dissolved in PEG-400 at 1 ml/kg. In the inset, the data for the NAc are averaged in 30 min blocks after injection (first: samples 1–3; second: samples 4–6; third: samples 7–9), to highlight the changes of the DA content for each experimental group. All data are expressed as means ± SEM. Range of basal levels of DA between groups in the NAc: 0.36 ± 0.05 to 0.93 ± 0.17 nM, in the VTA: 0.21 ± 0.08 to 0.50 ± 0.07 nM. Statistical analysis: in the *within*-group comparison of NAc data (panel A; one-way ANOVA), the vehicle group was non-significant, the 2.5 mg/kg group yielded $F(9, 69) = 9.607$, $p < 0.001$, the 5 mg/kg group $F(9, 59) = 5.601$, $p < 0.001$, and the 10 mg/kg group $F(9, 69) = 7.382$, $p < 0.001$. In the main plot, the shades of grey on the asterisks match the appropriate line graph and indicate significant difference from baseline (sample-1), using the Holm–Sidak test performed after the one-way ANOVA. In the inset, the crosses indicate significant difference from vehicle condition. *Between*-group comparison of NAc data (two-way ANOVA) yielded $F(6, 83) = 3.068$, with $p = 0.013$. For VTA data (B), both *within*-group and *between*-group comparisons were non-significant.

no additional stimulation of DA efflux was observed above the level produced with 5 mg/kg administration, and no higher doses were tested. The stimulation of DA efflux in the NAc appeared relatively rapid, peaking within 20 min (Fig. 2A). The levels of DA observed within the NAc after the i.p. injections of NP078585 were statistically different from both baseline and from levels in the presence of vehicle only (2.5 ml PEG-400; see legend to Fig. 2 for details). In contrast, all three doses of NP078585 produced no statistically significant effects on somatodendritic levels of DA within the VTA (Fig. 2B). Similar to that for the NAc, vehicle injections (2.5 ml PEG-400) did not significantly affect DA efflux from the VTA (Fig. 2A, B).

3.2. Role of N-type channels in NP078585-induced DA efflux in the Nucleus Accumbens

NP078585 is a potent, state-dependent blocker of N-type calcium channels (Snutch et al., 2001a, 2003), which play a major role in excitation–secretion coupling at central synapses (Dunlap et al., 1995). As such, NP078585 application was expected to produce either a depression or no change of DA efflux (Elverfors et al., 1997; but see Grilli et al., 1989), not the observed stimulation (see Fig. 2).

To investigate in more detail the mechanism of action of NP078585 and the role of N-type calcium channels in DA efflux, we applied NP078585 locally by reverse-dialysis within the mesocorticolimbic system, either to the VTA or to the NAc, and measured DA outflow from both sites in parallel. Application of NP078585 to the VTA at two different concentrations (10 μM and 25 μM, within the microdialysis probe) dose-dependently and rapidly enhanced DA levels within the NAc (Fig. 3A). A similar enhancement of accumbal DA efflux was seen following direct application of NP078585 to the NAc (10 μM; Fig. 3C). Similar to the systemic application experiments, intracerebral application of NP078585 produced a rapid stimulation of accumbal DA efflux,

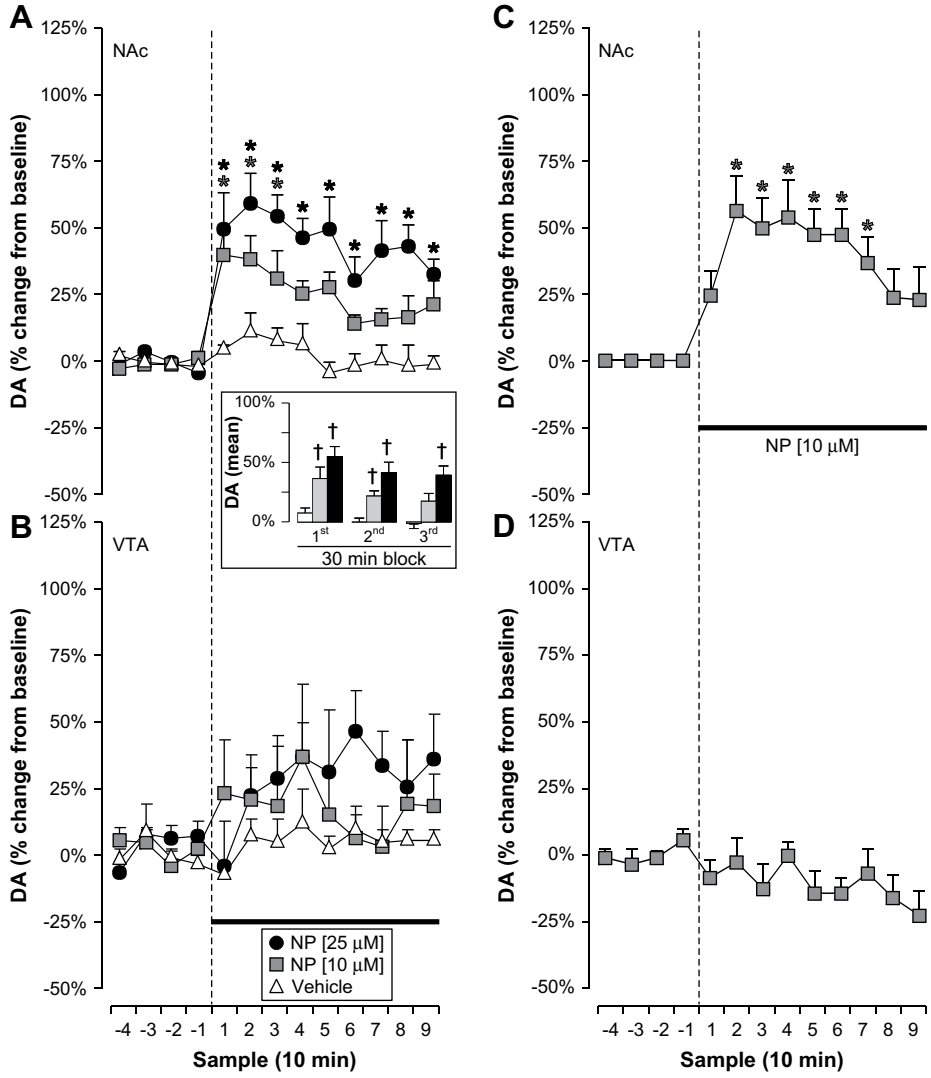

Fig. 3. Time-course of the change of DA efflux from the NAc (A, C) and the VTA (B, D), before and after dialysis of either NP078585 or vehicle (dashed lines). In (A) and (B), two concentrations of NP078585 (25 μM, black circles, $n = 7$; 10 μM, grey squares, $n = 9$ and $n = 8$, NAc and VTA, respectively) or vehicle (DMSO 0.5%, triangles, $n = 6$ and $n = 5$, NAc and VTA, respectively) were microdialyzed within the VTA (bar). In (C) and (D), only NP078585 (10 μM, $n = 7$ and $n = 5$, NAc and VTA, respectively) was microdialyzed within the NAc (bar). The dashed lines mark the start and the black bars duration (90 min) and site (NAc versus VTA) of the NP078585 or vehicle dialysis. The symbol NP stands for NP078585. Panels (A) and (B), range of basal levels of DA between groups in the NAc: 0.77 ± 0.42 to 2.20 ± 0.99 nM; in the VTA: 0.36 ± 0.09 to 0.59 ± 0.32 nM. Panels (C) and (D), basal levels of DA in the NAc: 1.11 ± 0.40 nM, in the VTA: 0.24 ± 0.06 nM. Statistical analysis: in the *within*-group comparison of NAc data (A; one-way ANOVA), the vehicle group was non-significant, the 10 μM group yielded $F(9, 89) = 2.782$, $p = 0.008$, the 25 μM group $F(9, 69) = 5.700$, $p < 0.001$. *Between*-group comparison of NAc data (A; two-way ANOVA) yielded $F(4, 65) = 3.068$, with $p = 0.013$. In the *within*-group comparison of NAc data (C), one-way ANOVA yielded $F(9, 69) = 4.719$ with $p < 0.001$. For VTA data (B, D), both *within*-group and *between*-group comparisons were non-significant. Other explanations are as in Fig. 2.

followed by a slow decay phase. The levels of DA observed in the NAc after reverse-dialysis of NP078585 (Fig. 3A, C) were statistically different from both baseline and from vehicle-associated levels, where available (see legend to Fig. 3). In contrast, extracellular levels of DA within the VTA were not significantly stimulated by NP078585 application to either the VTA itself (Fig. 3B) or to the NAc (Fig. 3D).

We next investigated whether the enhancements of DA efflux within the NAc could be accounted for by the N-type blocking action of NP078585. For this purpose we used the highly selective and potent cone snail peptide toxin, ω-conotoxin GVIA (Olivera et al., 1994). Similar to that for NP078585, reverse-dialysis of 2.5 μM ω-conotoxin enhanced DA efflux in NAc following VTA (Fig. 4A, B) or NAc (Fig. 4C) applications, and these same applications failed to affect DA levels within the VTA (Fig. 4B, D). The magnitude of DA efflux in the NAc following application of ω-conotoxin to either the VTA or NAc was statistically higher than baseline values before application, irrespective of its site of delivery (see legend to Fig. 4).

Thus both NP078585 and ω-conotoxin produced a moderate stimulation of basal DA efflux in the NAc, but not in the VTA, irrespective of whether their site of delivery was systemic (NP078585 only, Fig. 2), directly within the VTA (Fig. 3A, B and Fig. 4A, B) or into the NAc (Fig. 3C, D and Fig. 4C, D). The similarity of the effects of NP078585 and ω-conotoxin on DA efflux suggests a common mechanism, namely blockade of N-type calcium channels. We next tested the hypothesis that the main function of N-type channels in the mesocorticolimbic system is to gate inhibitory pathways regulating accumbal DA release.

3.3. Role of GABAergic and DAergic inhibitory pathways in mesocorticolimbic N-type function

Mesocorticolimbic dopaminergic neurons receive two major inhibitory inputs within the VTA, one from GABAergic neurons (Grace and Onn, 1989; Johnson and North, 1992) and the other auto-inhibitory, from the dendritic release of DA (Björklund and Lindvall, 1975; Geffen et al., 1976). Release of GABA requires

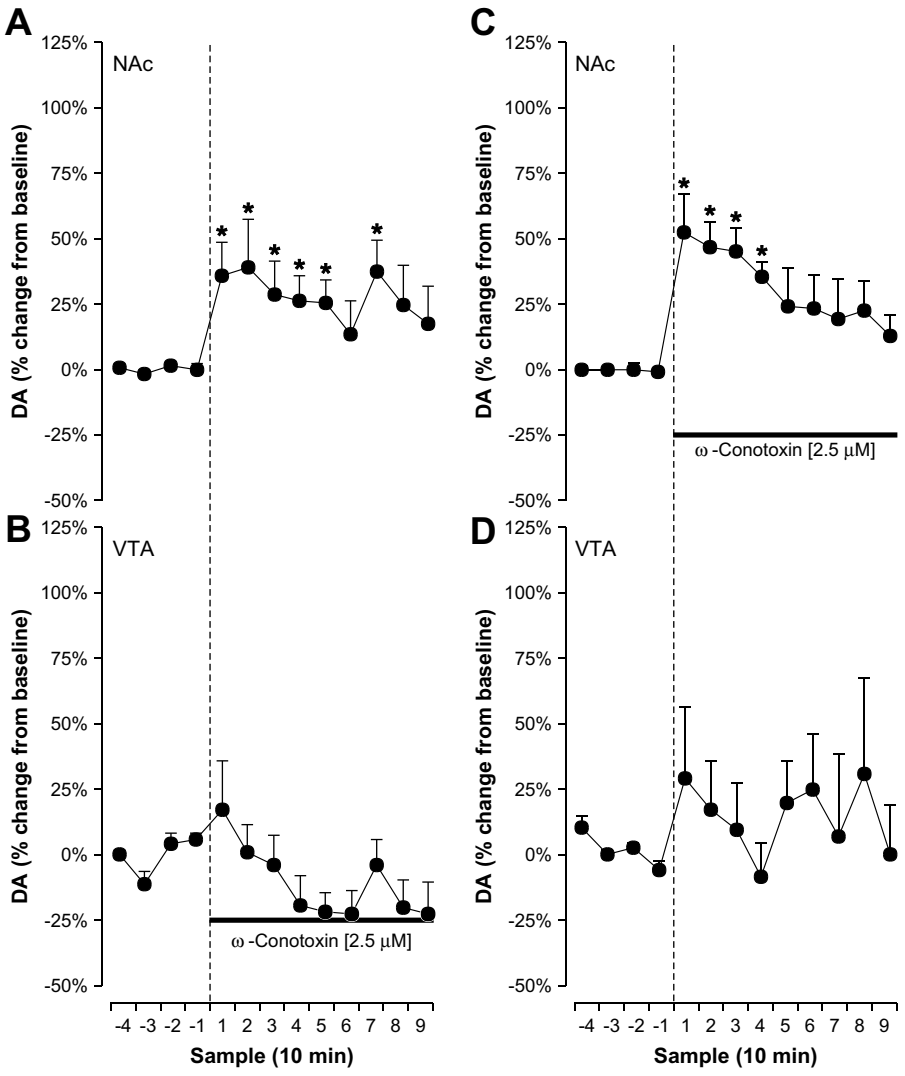

Fig. 4. Time-course of the change of DA efflux from the NAc (A, C) and the VTA (B, D), before and after reverse-dialysis of ω-conotoxin GVIA (dashed lines). In (A) and (B), ω-conotoxin GVIA (2.5 μM; $n = 6$ and $n = 7$, NAc and VTA, respectively) was microdialyzed within the VTA (bar). In (C) and (D), ω-conotoxin GVIA (2.5 μM; $n = 9$ and $n = 7$, NAc and VTA, respectively) was microdialyzed within the NAc (bar). Panels A and B, basal levels of DA in the NAc: 0.90 ± 0.20 nM; in the VTA: 0.41 ± 0.08 nM. Panels (C) and (D), basal levels of DA in the NAc: 1.12 ± 0.23 nM, in the VTA: 0.12 ± 0.04 nM. Statistical analysis: In the *within*-group comparison of NAc data (A), one-way ANOVA yielded $F(9, 59) = 3.090$ with $p = 0.006$. In the *within*-group comparison of NAc data (C), one-way ANOVA yielded $F(9, 89) = 5.615$ with $p < 0.001$. For VTA data (panels B, D), *within*-group comparisons were non-significant. Other explanations are as in Figs. 2 and 3.

voltage-gated calcium channel activity, while dendritic DA release appears to be largely calcium-independent (Bergquist et al., 1998; Dobrev et al., 1999; Phillips and Stamford, 2000; Chen et al., 2006). We first tested the hypothesis that suppression of the GABAergic input by NP078585 contributes to the observed accumbal stimulation of DA. Application of bicuculline to the VTA (50 μM) produced a large and sustained enhancement of DA efflux in both VTA and NAc (Fig. 5A, B: squares). These findings confirm previous observations of a robust role of GABA inhibition in the regulation of mesocorticolimbic DA efflux, in part via $GABA_A$ receptors (Westerink et al., 1996; Cobb and Abercrombie, 2002). If the potentiation produced by NP078585 of accumbal DA efflux (Figs. 2 and 3) is mediated through suppression of GABA release, it should be occluded by bicuculline. We tested this hypothesis by applying 50 μM bicuculline together with 10 μM NP078585. As shown in Fig. 5 (A, B: circles), no additional stimulation of accumbal DA efflux was observed after administration of NP078585. In both VTA and NAc, the levels of DA after bicuculline with or without NP078585 were significantly different from baseline ($p < 0.001$, one-way ANOVA), whereas there was no significant difference between the groups treated with bicuculline alone and those treated with bicuculline and NP078585. These data are consistent with the hypothesis that NP078585 acts on accumbal DAergic function upstream of GABA release, presumably by blocking N-type channels in GABAergic terminals. This event would lead to suppression of GABA release, which in turn removes an inhibitory input on dopaminergic cells leading to the observed increase of DA efflux from the NAc (see Fig. 7A).

We next tested the hypothesis that suppression of auto-inhibitory dendritic release of DA by NP078585 may also account for the enhancement of accumbal efflux of DA produced by N-type block. Application of haloperidol (100 μM) to the VTA enhanced dendritic

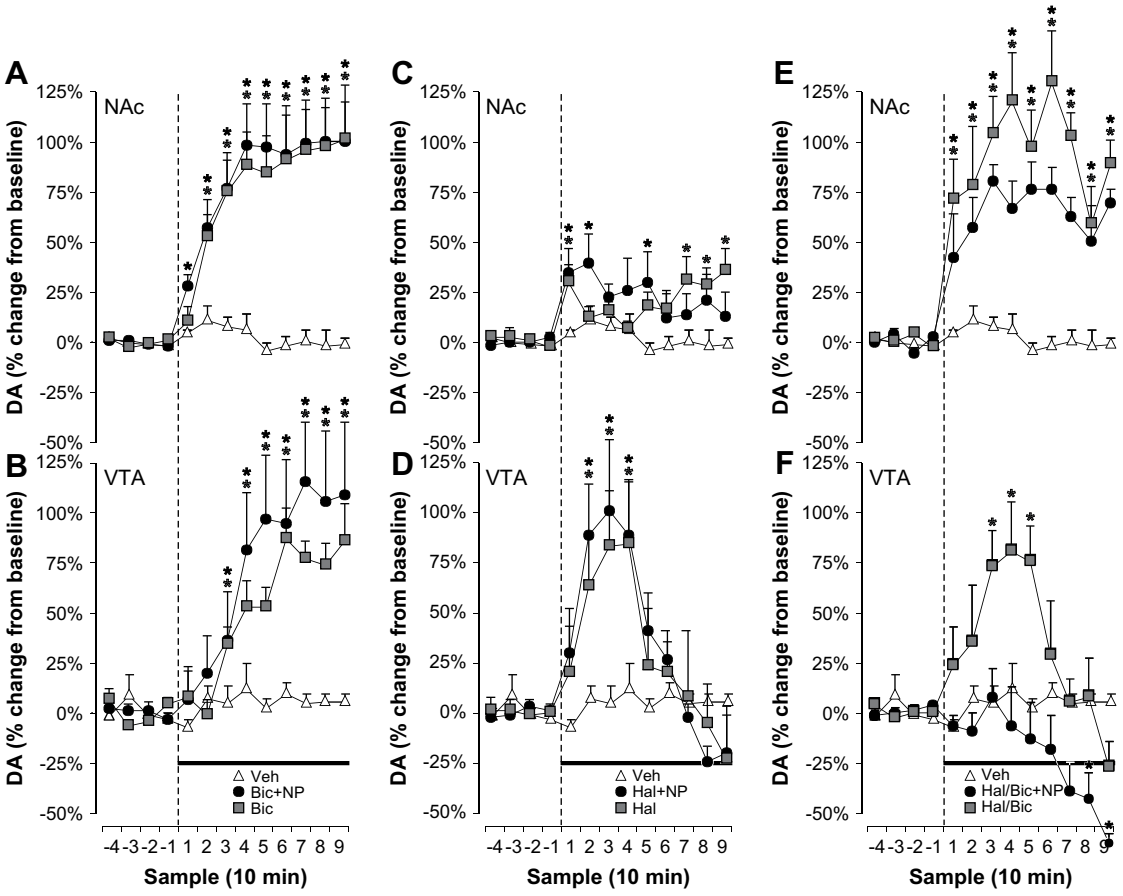

Fig. 5. Time-course of the change of DA efflux from the NAc (A, C and E) and the VTA (B, D and F), before and after three distinct groups of treatments (A to B, C to D, E to F; dashed lines). In (A) and (B), bicuculline was reverse-dialyzed in the VTA (50 μM; Bic, bar), in the presence (circles, $n = 11$; basal levels of DA in the NAc: 2.17 ± 0.75 nM; in the VTA: 0.56 ± 0.17 nM) or the absence (squares, $n = 8$; basal levels of DA in the NAc: 3.4 ± 0.84 nM; in the VTA: 0.18 ± 0.03 nM) of NP078585 (10 μM). In (C) and (D), haloperidol (100 μM; Hal, bar) was reverse-dialyzed in the same site, in the presence (circles, $n = 6$; basal levels of DA in the NAc: 1.25 ± 0.42 nM; in the VTA: 0.22 ± 0.07 nM) or the absence (triangles; $n = 8$ and $n = 7$, basal DA levels 1.02 ± 0.38 nM and 0.19 ± 0.09 nM, NAc and VTA, respectively) of NP078585 (10 μM). In (E) and (F) both bicuculline and haloperidol were reverse-dialyzed at the same concentrations in the same site, in the presence (circles, $n = 6$; basal levels of DA in the NAc: 1.64 ± 0.51 nM; in the VTA: 0.54 ± 0.15 nM) or the absence (squares; $n = 5$ and $n = 6$, basal DA levels 0.79 ± 0.23 nM and 0.30 ± 0.08 nM, NAc and VTA, respectively) of NP078585 (10 μM). The vehicle condition (intra-VTA reverse-dialysis of DMSO 0.5%, triangles, $n = 5$) is also shown in each of the three conditions. Statistical analysis, (A) In the *within*-group comparison of NAc data, the bicuculline alone group yielded $F(9, 79) = 7.898$, bicuculline plus NP078585 $F(9, 79) = 12.715$, both with $p < 0.001$. In the *between*-group comparisons, the differences were not significant. (B) In the *within*-group comparison of VTA data, the bicuculline alone group yielded $F(9, 79) = 9.495$, bicuculline plus NP078585 $F(9, 79) = 10.811$, both with $p < 0.001$. In the *between*-group comparisons, the differences were not significant. (C) In the *within*-group comparison of NAc data, the haloperidol alone group yielded $F(9, 79) = 3.516$, with $p = 0.001$ and haloperidol plus NP078585 $F(9, 59) = 2.745$, with $p = 0.012$. In the *between*-group comparisons, two-way ANOVA yielded $F(2, 41) = 4.573$ with $p = 0.018$. (D) In the *within*-group comparison of VTA data, the haloperidol alone group yielded $F(9, 69) = 7.701$, haloperidol plus NP078585 $F(9, 59) = 6.279$, both with $p < 0.001$. In the *between*-group comparisons, the differences were not significant. (E) In the *within*-group comparison of NAc data, the bicuculline and haloperidol alone group yielded $F(9, 59) = 5.289$, bicuculline and haloperidol plus NP078585 $F(9, 59) = 4.918$, both with $p < 0.001$. In the *between*-group comparisons, the differences were not significant. (F) In the *within*-group comparison of VTA data, the bicuculline and haloperidol alone group yielded $F(9, 59) = 5.083$, bicuculline and haloperidol plus NP078585 $F(9, 59) = 7.848$, both with $p < 0.001$. In the *between*-group comparisons, test of the main effect of conditions yielded $F(1, 10) = 6.414$ with $p = 0.03$. Other explanations are as in Figs. 2 and 3.

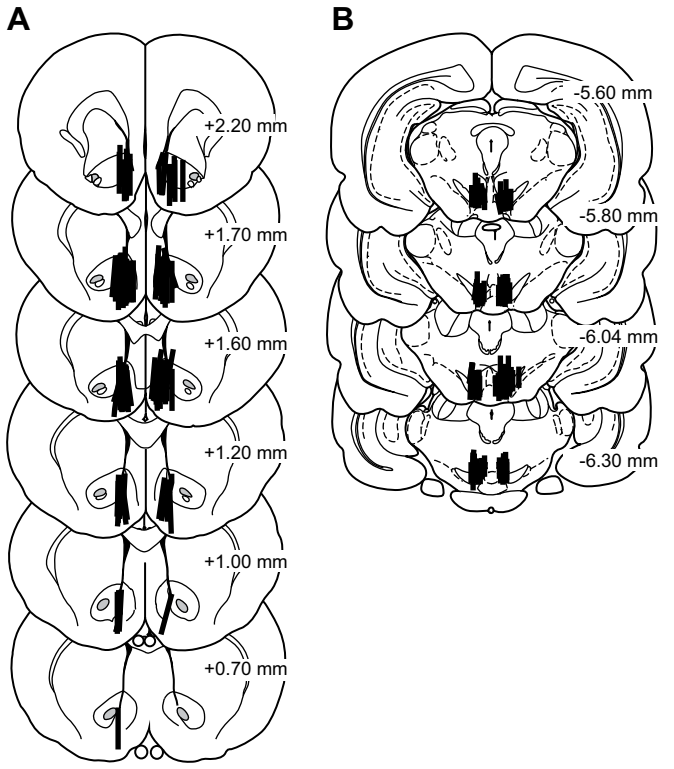

Fig. 6. Location of microdialysis probes in the NAc (A) and VTA (B). Vertical lines represent the semi-permeable membrane portion of microdialysis probes (2 mm length in the NAc and 1 mm length in the VTA; 300 μm outer diameter). Drawings of coronal sections were adapted from Paxinos and Watson (1997). Distance from bregma is indicated.

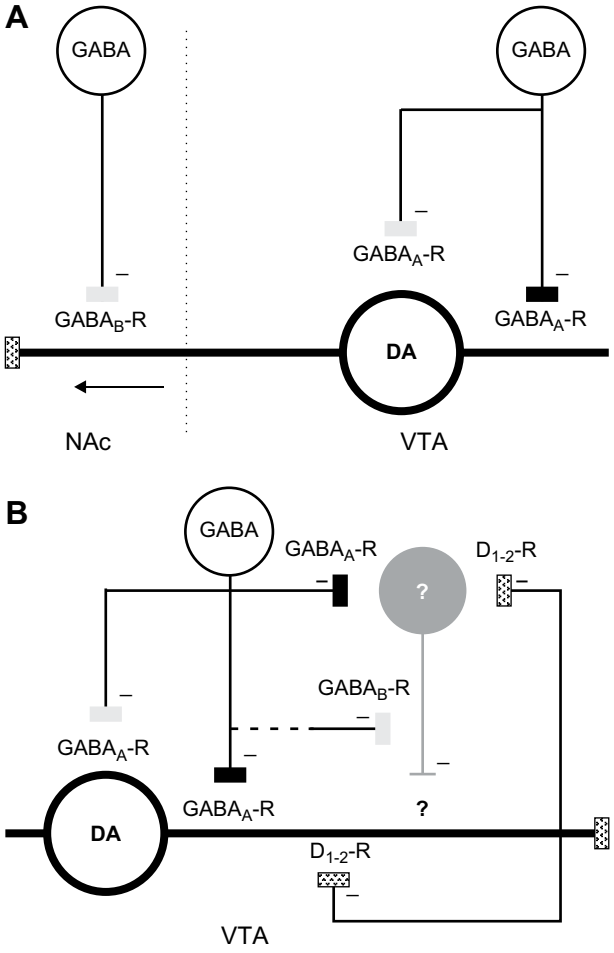

Fig. 7. Summary of the proposed mechanisms for control of DA release. In (A), regulation of DA release from the NAc, a process under the influence of mechanisms both in the VTA and the NAc itself. In (B), regulation of dendritic DA release within the VTA. In light grey, N-type dependent terminals. In black, N-type independent sites. Stippled, DAergic release sites. The question mark denotes an unknown mechanism and/or cellular pathway leading to depression of dendritic DA release.

DA efflux (Fig. 5D, squares), by a peak amount comparable to that produced by bicuculline in the same structure (Fig. 5B, same symbol). This is presumably due to the removal of a DA-mediated, local inhibitory feedback, leading to the simultaneous uncovering of excitatory inputs and/or endogenous DA release. However, in contrast to bicuculline, this enhancement was not accompanied by a parallel increase of DA efflux in the NAc (Fig. 5, compare panels A and C: squares). The latter observation suggests that dendritic autoinhibition plays a limited role in controlling distal release of DA within the NAc. Furthermore, NP078585 (10 μM) applied in combination with haloperidol to the VTA did not alter significantly the haloperidol-stimulated efflux of DA within the same structure (Fig. 5D, compare circles with squares), and stimulated the efflux of DA within the NAc above the level observed during applications of haloperidol alone, at least in the first hour (Fig. 5C: compare circles with squares). Importantly, NP078585 in combination with haloperidol enhanced DA efflux in the NAc essentially by the same amount as NP078585 alone at the same concentration, 10 μM (compare Fig. 5C circles with Fig. 3A, squares). In the VTA, DA levels after haloperidol with or without NP078585 were significantly different from baseline ($p < 0.001$, one-way ANOVA), whereas there was no significant difference between the groups treated with haloperidol alone and those treated with haloperidol and NP078585. In the NAc, the differences within groups and between groups were both statistically different ($p \leq 0.018$, one-way and two-way ANOVA, respectively).

In order to examine the mechanisms of dendritic DA efflux in the absence of both inhibitory mechanisms, we applied bicuculline (50 μM) and haloperidol (100 μM) in combination to the VTA, and measured DA efflux from the VTA itself and as well as from the NAc. We observed a robust surge of DA efflux at both sites (Fig. 5E, F, squares), similar in the VTA to that produced by haloperidol alone in the same site (Fig. 5D, squares) and in the NAc by bicuculline alone (Fig. 5A, squares). The levels of DA in both the VTA and the NAc after haloperidol and bicuculline in combination were significantly different from those observed in their respective baselines, ($p < 0.001$, one-way ANOVA). When NP078585 was applied to the VTA at 10 μM together with bicuculline and haloperidol, we observed a progressive and substantial decline of dendritic DA efflux in the VTA that contrasted with the maintained enhancement of DA efflux observed in the NAc (Fig. 5F, E, circles). The levels of DA after haloperidol, bicuculline and NP078585 were significantly different from baseline ($p < 0.001$, one-way ANOVA) in both VTA and NAc. However, in the VTA the difference between groups became significant ($p = 0.03$, two-way ANOVA), while in the NAc it failed to reach statistical significance.

4. Discussion

4.1. Block of calcium channels stimulates accumbal efflux of DA

We have shown that i.p. administration of the mixed N- and T-type calcium blocker NP078585 (2.5–10 mg/kg) rapidly and dose-dependently produces brain levels sufficient to block a large

fraction of these channels. Similar administration in parallel *in vivo* dialysis experiments triggered a fast enhancement of DA efflux in the NAc, but not in the VTA. It is important to recognize the slow temporal and limited spatial resolution of this sampling method and accordingly, it will be of interest to extend these findings with electrochemical and electrophysiological recording techniques. The enhanced and selective outflow of DA in the NAc was replicated by *in situ* application of either NP078585 or ω-conotoxin GVIA, which strongly implicates local N-type calcium channels in DA release. The *in situ* applications used concentrations of NP078585 and ω-conotoxin GVIA about two orders of magnitude larger than the IC_{50} of the target N-type channels. This was necessary to create a diffusion gradient across the semi-permeable membrane of the probe and the local brain tissue of sufficient strength to counterbalance the washout from the brain capillary circulation, as well as nonspecific protein and membrane binding. Due to this gradient imparted by the reverse-dialysis, N- and T-type calcium channels of neurons close to the microdialysis probe were presumably largely blocked. Furthermore, it may be assumed that those in the surrounding tissue were blocked by an average extent comparable to that observed during systemic application of NP078585. The observed coupling between channel blockade and DA enhancement is efficient, because block of an estimated 31% of N-type channels by 50 nM NP078585 in the brain 0.5 h after a 2.5 mg/kg dose is sufficient to produce a 60% increase of DA efflux, above its baseline (systemic administration, Fig. 2). Moreover, this level is near-maximal, since a fourfold larger dose of NP078585 produced 286 nM in the brain at 0.5 h (predicted to block ~70% of the channels), but resulted in only a modestly larger DA stimulation of 80% (Fig. 2). These data suggest that a limiting brain penetration of NP078585 is unlikely to account for the observed plateau of the DA enhancement. Rather, this plateau is most likely due to the net balance of the multiple mechanisms controlling DA release in the whole brain, one of which is likely N-type calcium channel-dependent.

The unexpected enhancement of DA efflux suggests that the *dominant* role of N-type channels in the mesocorticolimbic system may not involve direct control of accumbal DA release, as block of this class of calcium channel is expected to inhibit transmitter release. These data raise the question of the precise role played by N-type calcium channels. A possible answer is provided by the observation that in the VTA block of $GABA_A$ enhances DA efflux in the NAc (Bergquist et al., 1998; Dobrev et al., 1999; Phillips and Stamford, 2000; Chen et al., 2006), and that this enhancement prevented the potentiating effect of NP078585 on the accumbal DA efflux. This occlusion effect is not likely due to saturation of DA output following the removal of the $GABA_A$-induced inhibition, since DAergic terminals in the NAc can sustain much higher levels of release (Darracq et al., 2001; You et al., 2001; Kuroki et al., 2003; Peleg-Raibstein and Feldon, 2006). Thus NP078585 appears to act primarily at the level of the GABAergic neurons, presumably by reducing synaptic GABA release or the upstream excitatory inputs to these interneurons, or both. If that is the case, NP078585 functionally replicates the effects of opioids (Johnson and North, 1992). A similar mechanism may underlie the effect of NP078585 and ω-conotoxin GVIA applied directly to the NAc (Fig. 5A; Rahman and McBride, 2002; Akiyama et al., 2004).

NP078585 also blocks T-type calcium channels, albeit somewhat less potently than N-type channels. In thalamic GABAergic interneurons, burst activity and GABA secretion require T-type channel activity (Huguenard and Prince, 1992; Joksovic et al., 2005). If a similar mechanism is present in a subset of GABA interneurons of VTA, block of T-type channels by NP078585 could have inhibited burst-dependent GABA efflux and thus contributed to the disinhibition of dopaminergic neurons and the enhancement of DA efflux

4.2. Regulation of dendritic and accumbal release of DA can be dissociated

A second important finding emerging from the present work is the pharmacological dissociation of mechanisms regulating DA release in the NAc and the VTA. While either bicuculline or haloperidol produces similarly large increases of DA efflux within the VTA, only bicuculline simultaneously stimulates a distal efflux of DA in the NAc (Fig. 5A–D). Thus, a reduction in somatodendritic autoinhibition of DA neurons in the VTA is not propagated to the terminal regions, in contrast to the effect of local GABAergic disinhibition by bicuculline. This difference may reflect the fact that GABAergic, but not dopaminergic, disinhibition triggers critical changes in action potential activity in dopaminergic axons, thus accounting for NAc enhanced DA efflux. Further, these intra-VTA stimulatory effects of bicuculline and haloperidol are not mimicked or significantly affected by NP078585 applied alone (Fig. 3). These observations are crucial since they shed light on the role of both GABA and DA release mechanism in the VTA. In fact, persistence of haloperidol-induced efflux of DA within the VTA in the presence of NP078585 reinforces the notion that dendritic DA release does not rely on N-type calcium channels (Chen et al., 2006), and is more likely due to reversal of the DA transporter (Falkenburger et al., 2001; Kahlig et al., 2005). Further, the observation that bicuculline application stimulates DA efflux in the VTA, while NP078585 does not, suggests that GABAergic inhibition of dendritic release is insensitive to NP078585, presumably because GABA secretion is independent from N-type (and also T-type) calcium channel activity. This is in contrast with the proposed involvement of N-type (and possibly T-type: see Section 4.1) channels in a GABAergic mechanism controlling distal DA release in the NAc. Thus, it appears that within the VTA, two sets of GABAergic actions are at work on the same neuronal target, one N-type (and possibly T-type) sensitive regulating distal release of DA, the other N- and T-type insensitive, regulating local release (Fig. 7A). This is unlikely to be a unique or unusual arrangement as this phenomenon has been detected in the hippocampus (Poncer et al., 1997).

It is unclear why the effects of bicuculline on DA efflux are sustained within the time frame of the experiment (Fig. 5A, B), whereas those of haloperidol are transient (Fig. 5D) and those of NP078585 display an intermediate kinetic profile (see for example Fig. 3A, C). Presumably, $GABA_A$ receptor blockade can radically suppress mechanisms downregulating DA release and does not allow any compensatory feedback to take place, which may be at play with the more selective and/or local actions of NP078585 or haloperidol. Haloperidol has been shown to be also a modest blocker of N-type ($IC_{50} > 100\ \mu M$; Zamponi, 1999) and a more potent one of T-type calcium channels ($IC_{50s} = 1.2–1.4\ \mu M$; Santi et al., 2002). However, these potential actions likely do not account for the observed effects of haloperidol on DA efflux since VTA-applied haloperidol does not replicate the action of NP078585, which blocks both N- and T-type channels in the sub-micromolar range (Snutch et al., 2001a, 2003; Newton et al., 2008).

A further unexpected finding from the present work is that simultaneous blockade of N-type channels, along with $GABA_A$ and D_{1-2} receptors, induces a profound depression of DA levels in the VTA, without substantially affecting the efflux of DA in the NAc (Fig. 5F). In the one instance, this finding reinforces the view that regulation of dendritic and axon terminal release can be dissociated. In another instance, a novel, dominant mechanism, which negatively controls DA levels within the VTA, may be suppressed independently by activity in any of three inputs: either the $GABA_A$ or D_{1-2} receptors or the N-type calcium channel (possibly via GABA release and $GABA_B$ receptors; Fig. 7B). Activity in only one of these inputs alone appears sufficient to allow (a) stable levels of DA in the

VTA *milieu*, and (b) the observed enhancement of dendritic DA efflux in response to suppression of inhibitory inputs. This mechanism could be contained within a cell type distinct from DA neurons, or inherent to DA neurons. Attractive candidates for the first hypothesis are a subset of glial cells, which could actively take-up DA within the VTA, unless they are inhibited by $GABA_A$, $GABA_B$, or D_{1-2} receptors (Inazu et al., 2003; De Melo Reis et al., 2008). It is less likely that the DA transporter in DA neurons can directly account for the observed data, since the direction of the neuronal transporter is voltage-dependent (Falkenburger et al., 2001; Kahlig et al., 2005). Thus the combined blocks of $GABA_A$, $GABA_B$ and D_{1-2} receptors in the DA neuron itself should promote membrane depolarization and in turn enhance DA levels, not the opposite, as observed here (Fig. 5F: filled symbols).

4.3. Block of N-type calcium channels as a candidate target for drug dependency

Drugs producing elevated stimulation of central DA release can induce potent dependency (Wise, 2005). Indeed, this broad set of pharmacological observations has been instrumental in developing current ideas concerning the role of DA in reward and motivation (Fibiger and Phillips, 1988; Tamminga and Carlsson, 2002). We have shown that within the mesocorticolimbic dopaminergic system, NP078585 behaves functionally like a DA partial agonist, because it produces a moderate and self-limiting stimulation of accumbal efflux of DA (Tamminga and Carlsson, 2002). This property might be exploited for the clinical treatment of drug dependency (see Ohlsen and Pilowsky, 2005). Similarly, the $GABA_B$ agonist baclofen also produces moderate stimulation of DA neurons (Cruz et al., 2004) and is presently being investigated for the treatment of drug dependency (Cousins et al., 2002). Here we identify blockade of N-type calcium channels as a distinct, novel means to induce moderate stimulation of DA release, which is presumably devoid of the side effects of $GABA_B$ stimulation. This approach has been further validated by the recent observation in rodents that NP078585 reduces reward from ethanol in both operant self-administration and conditioned place preference, and importantly also reduces stress-induced reinstatement of ethanol drinking (Newton et al., 2008). Our findings may also have broader implications. For example, genetic ablation of N-type channels in mice is mildly anxiolytic (Saegusa et al., 2001), and fear conditioning requires the mesocorticolimbic DA system (Pezze and Feldon, 2004). Thus, any therapeutic action of N-type blockers in drug dependency may be in part supported by modulation of its affective components. Similarly, the well-established efficacy of N-type block in analgesia/anti-hyperalgesia (Snutch, 2005; Schroeder et al., 2006) could be in part explained by the involvement of the DA system (Wood, 2006), particularly regarding the affective/saliency aspects of the pain perception.

Acknowledgements

This project was supported by an Industry/University grant from the Canadian Institutes of Health Research (CHIR) to Neuromed Pharmaceuticals and A.G.P. T.P.S. is supported by an operating grant from CIHR (#10677) and a Tier 1 Canada Research Chair in Biotechnology and Genomics-Neurobiology. The authors are indebted to G. Vacca for collecting preliminary data, and to Ms. Diana Janke for technical support.

References

Akiyama, G., Ikeda, H., Matsuzaki, S., Sato, M., Moribe, S., Koshikawa, N., Cools, A.R., 2004. $GABA_A$ and $GABA_B$ receptors in the nucleus accumbens shell differentially modulate dopamine and acetylcholine receptor-mediated turning behaviour. Neuropharmacology 46, 1082–1088.

Bergquist, F., Jonason, J., Pileblad, E., Nissbrandt, H., 1998. Effects of local administration of L-, N-, and P/Q-type calcium channel blockers on spontaneous dopamine release in the striatum and the substantia nigra: a microdialysis study in rat. J. Neurochem. 70, 1532–1540.

Björklund, A., Lindvall, O., 1975. Dopamine in dendrites of substantia nigra neurons: suggestions for a role in dendritic terminals. Brain Res. 83, 531–537.

Catterall, W.A., 2000. Structure and regulation of voltage-gated Ca^{2+} channels. Ann. Rev. Cell. Dev. Biol. 16, 521–555.

Chen, B.T., Moran, K.A., Avshalumov, M.V., Rice, M.E., 2006. Limited regulation of somatodendritic dopamine release by voltage-sensitive Ca^{2+} channels contrasted with strong regulation of axonal dopamine release. J. Neurochem. 96, 645–655.

Cobb, W.S., Abercrombie, E.D., 2002. Distinct roles for nigral GABA and glutamate receptors in the regulation of dendritic dopamine release under normal conditions and in response to systemic haloperidol. J. Neurosci. 22, 1407–1413.

Cousins, M.S., Roberts, D.C., de Wit, H., 2002. $GABA_B$ receptor agonists for the treatment of drug addiction: a review of recent findings. Drug Alcohol Depend. 65, 209–220.

Cruz, H.G., Ivanova, T., Lunn, M.L., Stoffel, M., Slesinger, P.A., Luscher, C., 2004. Bi-directional effects of $GABA_B$ receptor agonists on the mesolimbic dopamine system. Nat. Neurosci. 7, 153–159.

Darracq, L., Drouin, C., Blanc, G., Glowinski, J., Tassin, J.P., 2001. Stimulation of metabotropic but not ionotropic glutamatergic receptors in the nucleus accumbens is required for the D-amphetamine-induced release of functional dopamine. Neuroscience 103, 395–403.

De Melo Reis, R.A., Ventura, A.L., Schitine, C.S., de Mello, M.C., de Mello, F.G., 2008. Müller glia as an active compartment modulating nervous activity in the vertebrate retina: neurotransmitters and trophic factors. Neurochem Res. 33, 1466–1474.

Dobrev, D., Milde, A.S., Andreas, K., Ravens, U., 1999. The effects of verapamil and diltiazem on N-, P- and Q-type calcium channels mediating dopamine release in rat striatum. Br. J. Pharmacol. 127, 576–582.

Dunlap, K., Luebke, J.I., Turner, T.J., 1995. Exocytotic Ca2+ channels in mammalian central neurons. Trends Neurosci. 18, 89–98.

Elverfors, A., Jonason, J., Jonason, G., Nissbrandt, H., 1997. Effects of drugs interfering with sodium channels and calcium channels on the release of endogenous dopamine from superfused substantia nigra slices. Synapse 26, 359–369.

Falkenburger, B.H., Barstow, K.L., Mintz, I.M., 2001. Dendrodendritic inhibition through reversal of dopamine transport. Science 293, 2465–2470.

Fallon, J.H., Moore, R.Y., 1978. Catecholamine innervation of the basal forebrain. IV. Topography of the dopamine projection to the basal forebrain and neostriatum. J. Comp. Neurol. 180, 545–580.

Fibiger, H.C., Phillips, A.G., 1988. Mesocorticolimbic dopamine systems and reward. Ann. N.Y. Acad. Sci. 537, 206–215.

Geffen, L.B., Jessell, T.M., Cuello, A.C., Iversen, L.L., 1976. Release of dopamine from dendrites in rat substantia nigra. Nature 260, 258–260.

Grace, A.A., Onn, S.P., 1989. Morphology and electrophysiological properties of immunocytochemically identified rat dopamine neurons recorded *in vitro*. J. Neurosci. 9, 3463–3481.

Grilli, M.G., Wright Jr., A.G., Hanbauer, I., 1989. Evidence for the involvement of distinct voltage-sensitive calcium channels in the release of ^{3}H-dopamine from primary cultures of mesencephalic neurons. Neuropharmacology 28, 1275–1278.

Huguenard, J.R., Prince, D.A., 1992. A novel T-type current underlies prolonged Ca^{2+}-dependent burst firing in GABAergic neurons of rat thalamic reticular nucleus. J. Neurosci. 12, 3804–3817.

Inazu, M., Takeda, H., Matsumiya, T., 2003. The role of glial monoamine transporters in the central nervous system. Nihon Shinkei Seishin Yakurigaku Zasshi 23, 171–178.

Johnson, S.W., North, R.A., 1992. Opioids excite dopamine neurons by hyperpolarization of local interneurons. J. Neurosci. 12, 483–488.

Joksovic, P.M., Brimelow, B.C., Murbartián, J., Perez-Reyes, E., Todorovic, S.M., 2005. Contrasting anesthetic sensitivities of T-type Ca^{2+} channels of reticular thalamic neurons and recombinant $Ca_{(v)}3.3$ channels. Br. J. Pharmacol. 144, 59–70.

Kahlig, K.M., Binda, F., Khoshbouei, H., Blakely, R.D., McMahon, D.G., Javitch, J.A., Galli, A., 2005. Amphetamine induces dopamine efflux through a dopamine transporter channel. Proc. Natl. Acad. Sci. U.S.A. 102, 3495–3500.

Kandel, E.R., 2000. Disorders of thought and volition: schizophrenia. In: Kandel, E.R. (Ed.), Principles of Neural Science. McGraw-Hill, New York, pp. 1188–1208.

Koob, G.F., 1992. Drugs of abuse: anatomy, pharmacology and function of reward pathways. Trends Pharmacol. Sci. 13, 177–184.

Kupfermann, I., Kandel, E.R., Iversen, S., 2000. Motivational and addictive states. In: Kandel, E.R. (Ed.), Principles of Neural Science. McGraw-Hill, New York, pp. 998–1018.

Kuroki, T., Meltzer, H.Y., Ichikawa, J., 2003. 5-HT 2A receptor stimulation by DOI, a 5-HT 2A/2C receptor agonist, potentiates amphetamine-induced dopamine release in rat medial prefrontal cortex and nucleus accumbens. Brain Res. 972, 216–221.

Newton, P.M., Orr, C.J., Wallace, M.J., Kim, C., Shin, H.S., Messing, R.O., 2004. Deletion of N-type calcium channels alters ethanol reward and reduces ethanol consumption in mice. J. Neurosci. 24, 9862–9869.

Newton, P.M., Zeng, L., Wang, V., Connolly, J., Wallace, M., Kim, C., Shin, H.-S., Belardetti, F., Snutch, T.P., Messing, R., 2008. A blocker of N- and T-type voltage-gated calcium channels attenuates ethanol-induced intoxication, place preference, self-administration, and reinstatement. J. Neurosci. 28, 11712–11719.

Olivera, B.M., Miljanich, G.P., Ramachandran, J., Adams, M.E., 1994. Calcium channel diversity and neurotransmitter release: the ω-conotoxins and ω-agatoxins. Annu. Rev. Biochem. 63, 823–867.
Ohlsen, R.I., Pilowsky, L.S., 2005. The place of partial agonism in psychiatry: recent developments. J. Psychopharmacol. 19, 408–413.
Paxinos, G., Watson, C., 1997. The Rat Brain in Stereotaxic Coordinates. Academic Press, London.
Peleg-Raibstein, D., Feldon, J., 2006. Effects of dorsal and ventral hippocampal NMDA stimulation on nucleus accumbens core and shell dopamine release. Neuropharmacology 51, 947–957.
Perez-Reyes, E., 2003. Molecular physiology of low-voltage-activated T-type calcium channels. Physiol. Rev. 83, 117–161.
Pezze, M.A., Feldon, J., 2004. Mesolimbic dopaminergic pathways in fear conditioning. Prog. Neurobiol. 74, 301–320.
Phillips, P.E., Stamford, J.A., 2000. Differential recruitment of N-, P- and Q-type voltage-operated calcium channels in striatal dopamine release evoked by 'regular' and 'burst' firing. Brain Res. 884, 139–146.
Poncer, J.-C., McKinney, R.A., Gahwiler, B.H., Thompson, S.M., 1997. Either N- or P-type calcium channels mediate GABA release at distinct hippocampal inhibitory synapses. Neuron 18, 463–472.
Rahman, S., McBride, W.J., 2002. Involvement of GABA and cholinergic receptors in the nucleus accumbens on feedback control of somatodendritic dopamine release in the ventral tegmental area. J. Neurochem. 80, 646–654.
Saegusa, H., Kurihara, T., Zong, S., Kazuno, A., Matsuda, Y., Nonaka, T., Han, W., Toriyama, H., Tanabe, T., 2001. Suppression of inflammatory and neuropathic pain symptoms in mice lacking the N-type Ca^{2+} channel. EMBO J. 20, 2349–2356.
Santi, C.M., Cayabyab, F.S., Sutton, K.G., McRory, J.E., Mezeyova, J., Hamming, K.S., Parker, D., Stea, A., Snutch, T.P., 2002. Differential inhibition of T-type calcium channels by neuroleptics. J. Neurosci. 22, 396–403.
Schroeder, C.I., Doering, C.J., Zamponi, G.W., Lewis, R.J., 2006. N-type calcium channel blockers: novel therapeutics for the treatment of pain. Med Chem. 2, 535–543.
Schultz, W., 2007. Behavioral dopamine signals. Trends Neurosci. 30, 203–210.
Snutch, T.P., 2005. Targeting chronic and neuropathic pain: the N-type calcium channel comes of age. NeuroRx 2, 662–670.
Snutch, T.P., Feng, Z.P., Doering, C., Cayabyab, F., Janke, D., Parker, D.B., Belardetti, F., Morimoto, B., Vanderah, T., Zamponi, G.W., Porreca, F., 2001a. A new class of N-type calcium channel blocker efficacious in animal models of chronic pain. Soc. Neurosci. 465.1.
Snutch, T.P., Sutton, K.G., Zamponi, G.W., 2001b. Voltage-dependent calcium channels–beyond dihydropyridine antagonists. Curr. Opin. Pharmacol. 1, 11–16.
Snutch, T., Feng, Z., Doering, C., Cayabyab, F., Janke, D., Parker, D., Belardetti, F., Morimoto, B., Venderah, B., Zamponi, G., Porreca, F., 2003. Novel N-type calcium channel blockers efficacious in animal models of chronic pain. In: 226th ACS National Meeting, Paper 6.
Snutch, T.P., Peloquin, J., Mathews, E., McRory, J., 2005. Molecular properties of voltage-gated calcium channels. In: Zamponi, G. (Ed.), Voltage-gated Calcium Channels. Landes Bioscience, New York, pp. 61–94.
Tamminga, C.A., Carlsson, A., 2002. Partial dopamine agonists and dopaminergic stabilizers, in the treatment of psychosis. Curr. Drug Targets CNS Neurol. Disord. 1, 141–147.
Vacca, G., Ahn, S., So, K., Snutch, T.P., Phillips, A.G., Belardetti, F., 2005. Block of N-type calcium channels stimulates the release of dopamine from rat mesolimbic neurons. Soc. Neurosci. Abs 265.2.
Westerink, B.H., Kwint, H.F., deVries, J.B., 1996. The pharmacology of mesolimbic dopamine neurons: a dual-probe microdialysis study in the ventral tegmental area and nucleus accumbens of the rat brain. J. Neurosci. 16, 2605–2611.
Wise, R.A., 2005. Forebrain substrates of reward and motivation. J. Comp. Neurol. 493, 115–121.
Wood, P.B., 2006. Mesolimbic dopaminergic mechanisms and pain control. Pain 120, 230–234.
Wolfart, J., Roeper, J., 2002. Selective coupling of T-type calcium channels to SK potassium channels prevents intrinsic bursting in dopaminergic midbrain neurons. J. Neurosci. 22, 3404–3413.
You, Z.B., Chen, Y.Q., Wise, R.A., 2001. Dopamine and glutamate release in the nucleus accumbens and ventral tegmental area of rat following lateral hypothalamic self-stimulation. Neuroscience 107, 629–639.
Zamponi, G.W., 1999. Cytoplasmic determinants of piperidine blocking affinity for N-type calcium channels. J. Membr. Biol. 167, 183–192.